The Astrophysical Journal, 574:356–363, 2002 July 20
© 2002. The American Astronomical Society. All rights reserved. Printed in U.S.A.

HYDROMAGNETIC INSTABILITIES IN PROTO–NEUTRON STARS

Juan A. Miralles,[1] José A. Pons,[2] and Vadim A. Urpin[3,4]
Received 2001 December 21; accepted 2002 March 26

ABSTRACT

The stability properties of newly born neutron stars, or proto–neutron stars (PNSs), are considered. We take into account dissipative processes, such as neutrino transport and viscosity, in the presence of a magnetic field. In order to find the regions of the star subject to different sorts of instability, we derive the general instability criteria and apply them to evolutionary models of PNSs. The influence of the magnetic field on instabilities is analyzed, and the critical magnetic field stabilizing the star is obtained. In light of our results, we estimate the maximum poloidal magnetic field that might be present in young pulsars or magnetars.

Subject headings: convection — instabilities — MHD — stars: magnetic fields — stars: neutron

1. INTRODUCTION

Neutron stars are born in the aftermath of core-collapse supernovae explosions, the fate of massive stars within a range of 8–30 $M_{\odot}$. In the final stages of stellar evolution, an iron core grows until electron captures or photodisintegration of heavy nuclei trigger its gravitational collapse. The collapse proceeds until nuclear density is reached and the stiffening of the equation of state provokes the bounce of the infalling material. A shock wave forms and propagates outward, leaving behind a newly born, hot, lepton-rich proto–neutron star (PNS). These objects are prodigious emitters of neutrinos of all types, which dominate the energetics of core-collapse supernovae and play a crucial role in the explosion mechanism by carrying away the binding energy from the PNS and depositing a part of it in the outer regions.

Whether or not the energy relocated by neutrinos is able to relaunch the stalled shock is still a controversial issue (Burrows et al. 2000; Rampp & Janka 2000; Janka 2000; Liebendorfer et al. 2001) that has led to speculation about alternative ways the explosion is powered, such as convection, rotation, and magnetohydrodynamic effects. In particular, it has been recognized by a number of authors that convective energy transport in the newly born PNS might play an important role by increasing the neutrino luminosity required to ignite the supernova explosion (Burrows & Fryxell 1993; Janka & Müller 1996; Bruenn & Dineva 1996). Convection in PNSs can be driven not only by the lepton gradient, as originally suggested by Epstein (1979), but also by the development of negative entropy gradients, which is common in many simulations of supernovae models (Bruenn & Mezzacappa 1994, 1995; Rampp & Janka 2000; Liebendorfer et al. 2001) and evolutionary models of PNSs (Burrows & Lattimer 1986; Keil & Janka 1995; Keil, Janka, & Müller 1996; Pons et al. 1999, 2001a, 2001b), despite differences in the equation of state and neutrino transport.

Although stellar core collapse may also have dramatic consequences on the magnetic field strength, the effect of magnetic fields was not considered in the above mentioned works, mainly because of the tough technical difficulties inherent to multidimensional magnetohydrodynamical simulations. It is known that the magnetic field in a collapsing star can be amplified by many orders of magnitude because of the conservation of the magnetic flux. This idea is often used to explain the origin of strong magnetic fields in neutron stars (Ginzburg 1964; Ginzburg & Ozernoy 1964; Woltjer 1964; Zeldovich & Novikov 1971; Shapiro & Teukolsky 1983). The conductivity of plasma inside the star is so large that the magnetic decay timescale is much shorter than the collapse time for a length scale of the magnetic field comparable to the stellar radius. Therefore, the field is frozen in, and the magnetic flux is conserved during the collapse stage. In the case of a frozen-in magnetic field, the average field strength increases approximately as $B \propto \rho^{2/3}$, where ρ is the density. By assuming that the magnetic field strength of the core of a massive star is comparable to that of strongly magnetized white dwarfs ($\sim 10^9$ G), at the end of core collapse, the neutron star may have a magnetic field $\sim 10^{13}$–10^{14} G, comparable to that observed in young radio pulsars. Following the same arguments, if we consider that the magnetic flux is conserved during the evolution of a massive star from the main sequence, starting from an initial magnetic field of $\sim 10^3$–10^4 G, we end up with a magnetic field of $\sim 10^{13}$–10^{14} G at the time the core of the star has become a neutron star. Similar arguments are often used to estimate the magnetic field of neutron stars formed from magnetized white dwarfs by the "accretion-induced collapse" mechanism. Note that these estimates give the order of magnitude of a poloidal field. The toroidal field, however, might be much stronger (Ardelyan, Bisnovatyi-Kogan, & Popov 1980).

Under certain conditions, convective motions in PNSs can amplify the magnetic field via dynamo action. The most optimistic estimates lead some authors (Thompson & Duncan 1993; Thompson & Murray 2001) to the conclusion that turbulent dynamo action could be responsible for the formation of ultramagnetized neutron stars (magnetars), with fields as strong as $\sim 10^{16}$ G at a very early evolutionary stage. Certainly, such strong magnetic fields influence magnetohydrodynamic processes in PNSs, particularly their stability properties. At this point, the fact that the convective overturn is intrinsically a three-dimensional phenom-

[1] Departament de Física Aplicada, Universitat d'Alacant, Apartat de Correus 99, E-03080 Alacant, Spain.
[2] Dipartimento di Fisica "G. Marconi," Università di Roma, La Sapienza, I-00184 Rome, Italy.
[3] Departament d'Astronomía i Astrofísica, Universitat de Valéncia, E-46100 Burjassot, Spain.
[4] A. F. Ioffe Institute of Physics and Technology, 194021 St. Petersburg, Russia.

enon makes fully consistent numerical simulations a very laborious and computationally expensive way to address the problem, and simplified semianalytical approaches are extremely useful for evaluating the necessity of more detailed studies. In this respect, some attempts have been made to establish definite criteria as to the different types of instability and their growth times (Bruenn & Dineva 1996; Miralles, Pons, & Urpin 2000, hereafter MPU00). In MPU00 we derived the general criteria for instability, taking dissipative processes into account such as neutrino transport and viscosity. In the present paper, we consider the stability properties of magnetic PNSs in detail. It is well known (see, e.g., Chandrasekhar 1961) that the magnetic field may stabilize a fluid against convection, causing an additional effective viscosity due to Lorentz force. On the other hand, the field can lead to new branches of instability associated, for instance, with Alfvén waves. In this paper, we present the main results of a general stability analysis in magnetized PNSs. The stability properties are considered for a wide range of magnetic fields.

The paper is organized as follows. In § 2 we obtain the dispersion equation that determines the condition of linear instability from the equations governing magnetohydrodynamics of PNSs and neutrino transport. In § 3 we discuss the stability properties of both nonmagnetic (§ 3.1) and magnetic (§ 3.2) PNSs, applying the criteria of hydromagnetic stability to the results of numerical simulations to identify the unstable zones. We also calculate the critical magnetic field that stabilizes a PNS. Finally, in § 4 we summarize and discuss our main findings.

2. THE DISPERSION EQUATION

Consider the stability properties on adopting a plane-parallel geometry. We assume that within the layer between $z = 0$ and $z = d$, the gravity $\boldsymbol{g}$ is directed in the negative z-direction and neglect the nonuniformity of $\boldsymbol{g}$ as well as general-relativistic corrections to the equations of hydrodynamics. The characteristic cooling timescale of a PNS is assumed to be much longer than the growth time of instability; thus, the latter can be treated in a quasi-stationary approximation. Since the convective velocities are typically much smaller than the speed of sound, one can describe instability by making use of the standard Boussinesq approximation (see, e.g., Landau & Lifshitz 1987). We consider the linear instability regime when the equations governing small perturbations can be obtained by the linearization of hydrodynamic equations. In the following, small perturbations of hydrodynamic quantities are marked by a subscript "1." For simplicity, the unperturbed magnetic field is assumed to be vertical. The linearized momentum, continuity, and induction equations read

$$\rho\dot{\boldsymbol{v}}_1 = -\boldsymbol{\nabla}p_1 + \boldsymbol{g}\rho_1 + \frac{1}{4\pi}(\boldsymbol{\nabla}\times\boldsymbol{B}_1)\times\boldsymbol{B} + \rho\nu\Delta\boldsymbol{v}_1 \ , \quad (1)$$

$$\boldsymbol{\nabla}\cdot\boldsymbol{v}_1 = 0 \ , \quad (2)$$

$$\dot{\boldsymbol{B}}_1 = \boldsymbol{\nabla}\times(\boldsymbol{v}_1\times\boldsymbol{B}) + \nu_m\Delta\boldsymbol{B}_1 \ , \quad (3)$$

$$\boldsymbol{\nabla}\cdot\boldsymbol{B}_1 = 0 \ , \quad (4)$$

where p and ρ are the pressure and density, respectively, ν is the viscosity, and ν_m is the magnetic diffusivity. We assume that the matter inside a PNS is in chemical equilibrium; thus, the density can generally be considered as a function of the pressure p, temperature T, and lepton fraction $Y = (n_e + n_\nu)/n$, with n_e and n_ν being the net (particles minus antiparticles) number densities of electrons and neutrinos, respectively, and $n = n_p + n_n$ being the number density of baryons. Then, the perturbations of density, entropy per baryon (s), and neutrino chemical potential (μ) can be expressed in terms of p_1, T_1, and Y_1. In the Boussinesq approximation, the perturbations of pressure are negligible because the fluid motions are assumed to be slow and the moving fluid elements are nearly in pressure equilibrium with their surroundings. Therefore, we have

$$\rho_1 \approx -\rho\left(\beta\frac{T_1}{T} + \delta Y_1\right) \ , \quad (5)$$

$$s_1 \approx m_p c_p\frac{T_1}{T} + \sigma Y_1 \ , \quad (6)$$

where m_p is the proton mass (we neglect the mass difference between protons and neutrons), β and δ are the coefficients of thermal and chemical expansion, respectively [$\beta = -(\partial\ln\rho/\partial\ln T)_{pY}$, $\delta = -(\partial\ln\rho/\partial Y)_{pT}$], $\sigma = (\partial s/\partial Y)_{pT}$, and $c_p = (T/m_p)(\partial s/\partial T)_{pY}$ is the specific heat at constant pressure.

The above equations should be complemented by the equation driving the evolution of chemical composition and heat balance. We employ the equilibrium diffusion approximation, which is sufficiently accurate and reliable during the early stage of PNS evolution, when the mean free path of a neutrino is short compared to the density and temperature length scales. In this approximation, the diffusion and thermal balance equations can be linearized (see MPU00 for details) and written as

$$\dot{Y}_1 + \boldsymbol{v}_1\cdot\boldsymbol{\nabla}Y = \lambda_T\frac{\Delta T_1}{T} + \lambda_Y\Delta Y_1 \ , \quad (7)$$

$$\frac{\dot{T}_1}{T} - \boldsymbol{v}_1\cdot\frac{\Delta\boldsymbol{\nabla}T}{T} = \kappa_T\frac{\Delta T_1}{T} + \kappa_Y\Delta Y_1 \ , \quad (8)$$

where

$$\Delta\boldsymbol{\nabla}T \equiv -\frac{T}{m_p c_p}(\boldsymbol{\nabla}s - \sigma\boldsymbol{\nabla}Y) = \left(\frac{\partial T}{\partial p}\right)_{s,Y}\boldsymbol{\nabla}p - \boldsymbol{\nabla}T \quad (9)$$

is the superadiabatic temperature gradient, i.e., the difference between the temperature gradient of a fluid with constant entropy and composition and the actual temperature gradient, and the transport coefficients λ_T, κ_T, λ_Y, and κ_Y have been defined in MPU00.

Equations (1)–(4), (7), and (8), together with the corresponding boundary conditions, determine the behavior of small perturbations. For simplicity, we consider the case of vanishing perturbations at the boundaries $z = 0$ and $z = d$. Note that other boundary conditions cannot change the main conclusions of our analysis qualitatively.

Without loss of generality, the dependence of all perturbations on time and on the horizontal coordinate can be chosen as $\exp(\gamma t - ikx)$, where k is the horizontal wavevector and γ is a constant that can be complex, and its real part gives the inverse growth (or decay) timescale. Then, equations (1)–(4), (12), and (13) can be reduced to only one equa-

tion of higher order. Solving for v_{1z}, we obtain[5]

$$\Delta\left[(\gamma-\kappa_T\Delta)(\gamma-\lambda_Y\Delta)-\lambda_T\kappa_Y\Delta^2\right] \times\left[(\gamma-\nu\Delta)(\gamma-\nu_m\Delta)-c_{\rm A}^2\frac{d^2}{dz^2}\right]v_{1z} = gk^2\left\{\frac{dY}{dz}\left[\delta(\gamma-\kappa_T\Delta)+\beta\kappa_Y\Delta\right] -\frac{\Delta\nabla T}{T}\left[\beta(\gamma-\lambda_Y\Delta)+\delta\lambda_T\Delta\right]\right\}(\gamma-\nu_m\Delta)v_{1z}\ , \quad (10)$$

where $c_{\rm A}=B/(4\pi\rho)^{1/2}$ is the Alfvén velocity and $\Delta=d^2/dz^2-k^2$. The coefficients of this equation are constant in our simplified approach. The solution for the fundamental mode with "zero boundary conditions" has the form $v_{1z}\propto\sin(\pi z/d)$. Thus, the dispersion equation for the fundamental mode is

$$[(\gamma+\omega_\nu)(\gamma+\omega_m)+\omega_{\rm A}^2][(\gamma+\omega_T)(\gamma+\omega_Y)-\omega_{TY}\omega_{YT}] =(\gamma+\omega_m)\left[\omega_g^2(\gamma+\omega_Y-\alpha\omega_{YT})+\omega_L^2\left(\gamma+\omega_T-\frac{\omega_{TY}}{\alpha}\right)\right]\ , \quad (11)$$

where $\alpha=\delta/\beta$. In this expression, we introduced the characteristic frequencies

$$\omega_\nu=\nu Q^2,\quad \omega_m=\nu_m Q^2,\quad \omega_T=\kappa_T Q^2,\quad \omega_Y=\lambda_Y Q^2\ ,$$
$$\omega_{YT}=\lambda_T Q^2,\quad \omega_{TY}=\kappa_Y Q^2,\quad \omega_{\rm A}=\frac{c_{\rm A}\pi}{a}\ ,$$
$$\omega_g^2=\frac{\beta g k^2\Delta\nabla T}{TQ^2},\quad \omega_L^2=-\frac{\delta g k^2}{Q^2}\frac{dY}{dz}\ , \quad (12)$$

with $Q^2=(\pi/d)^2+k^2$. The quantities ω_ν, ω_m, ω_T, and ω_Y are the inverse timescales of dissipation of the perturbations due to viscosity, magnetic diffusivity, thermal conductivity, and chemical diffusivity, respectively; ω_{YT} characterizes the rate of diffusion caused by the temperature inhomogeneity (thermodiffusion), ω_{TY} describes the influence of chemical inhomogeneities on the rate of thermal evolution, ω_g is the frequency (or, in the case of instability, the inverse growth time) of the buoyant wave, ω_L characterizes the dynamical timescale of the processes associated with the lepton gradient, and $\omega_{\rm A}$ is the Alfvén frequency.

3. STABILITY OF PROTO–NEUTRON STARS

3.1. *Nonmagnetic PNSs*

Consider initially the case when $\boldsymbol{B}=0$. Then, equation (11) is reduced to a cubic equation with the roots given by

$$\gamma^3+a_2\gamma^2+a_1\gamma+a_0=0\ , \quad (13)$$

where

$$a_2=\omega_\nu+\omega_T+\omega_Y\ ,$$
$$a_1=\omega_T\omega_Y-\omega_{TY}\omega_{YT}+\omega_\nu(\omega_T+\omega_Y)-(\omega_g^2+\omega_L^2)\ ,$$
$$a_0=\omega_\nu(\omega_T\omega_Y-\omega_{TY}\omega_{YT}) -\omega_g^2(\omega_Y-\alpha\omega_{YT})-\omega_L^2\left(\omega_T-\frac{1}{\alpha}\omega_{TY}\right)\ . \quad (14)$$

[5] In the following, we use $\Delta\nabla T$ to denote its z-component.

Equation (13) describes three essentially different modes, corresponding to the three roots of the equation, which can generally exist in a chemically inhomogeneous fluid. The condition that at least one of the roots has a positive real part (unstable mode) is equivalent to one of the following inequalities,

$$a_2<0,\quad a_0<0,\quad a_1a_2<a_0\ , \quad (15)$$

being fulfilled (see, e.g., Aleksandrov, Kolmogorov, & Laurentiev 1985; DiStefano, Stubberud, & Williams 1994). Since κ_T and λ_Y are positive defined quantities, the first condition $a_2<0$ never applies, and only the two other conditions determine the stability of nonmagnetic PNSs.

Generally, the last two conditions in equation (15) are rather complex and depend on the horizontal wavevector of perturbations k. The critical temperature and lepton gradients that determine the transition from stability to instability can be quite different for perturbations with different k. In order to obtain the true criteria, we have to find the minimal values of these gradients that can cause instability. From the properties of the kinetic coefficients, we have $(\kappa_T\lambda_Y-\kappa_Y\lambda_T)>0$; therefore, the gradients in the last two conditions in equation (15) are minimal for perturbations with the wavevector k minimizing the quantity Q^6/k^2. This happens when $k^2=(\pi/d)^2/2$. For such a horizontal wavevector, the instability criteria read

$$\frac{dY}{dz}(\delta\kappa_T-\beta\kappa_Y)-\frac{\Delta\nabla T}{T}(\beta\lambda_Y-\delta\lambda_T) <-\frac{27\pi^4}{4gd^4}\nu(\kappa_T\lambda_Y-\kappa_Y\lambda_T)\ , \quad (16)$$

$$\frac{dY}{dz}[\delta(\nu+\lambda_Y)+\beta\kappa_Y]-\frac{\Delta\nabla T}{T}[\beta(\nu+\kappa_T)+\delta\lambda_T] <-\frac{27\pi^4}{4gd^4}(\kappa_T+\lambda_Y)[(\nu+\kappa_T)(\nu+\lambda_Y)-\lambda_T\kappa_Y]\ . \quad (17)$$

The conditions in equations (16) and (17) divide the $\Delta\nabla T$-∇Y plane into four regions that are characterized by different stability properties. The size and configuration of these regions depend on the thermodynamic and kinetic properties of nuclear matter. A detailed analysis of the stability of nonmagnetic PNSs based on the criteria in equations (16) and (17) has been done in MPU00. In that paper, as in the present one, we use results from numerical simulations of PNS evolution by Pons et al. (1999) to calculate the different thermodynamical derivatives, diffusion coefficients, and conductivities appearing in the stability criteria. To illustrate the large variety of situations encountered during the Kelvin-Helmholtz phase of a PNS, we have chosen three different cases. The physical conditions and the different transport parameters are summarized in Table 1. Case A corresponds to a layer near the center of the star, with an enclosed mass of 0.05 $M_\odot$ at an evolutionary time of $t=2$ s, when the PNS is in the deleptonization stage and the core is being heated. Cases B and C correspond to two different layers at a time of $t=20$ s during the cooling stage, mainly driven by thermal neutrinos since an important part of the lepton content of the star has already been radiated away. The layer corresponding to case B is located at the same depth as case A (0.05 $M_\odot$), while the layer in case C has an enclosed baryonic mass of 1 $M_\odot$. In our calculations, we have used the value of d given by the pressure height $d=l\equiv|d\ln p/dr|^{-1}$.

TABLE 1

PHYSICAL CONDITIONS AND TRANSPORT COEFFICIENTS FOR THREE REPRESENTATIVE SITUATIONS DURING THE FIRST SECONDS OF LIFE OF A PNS

	THERMODYNAMIC STATE					TRANSPORT COEFFICIENTS (cm)			
CASE	n_B (fm^{-3})	T (MeV)	Y_L	β	δ	κ_T	κ_Y	λ_T	λ_Y
A (stable)	0.301	21.1	0.333	0.103	0.111	0.556	−0.851	−0.046	0.496
B (convection).....	0.350	33.6	0.259	0.145	−0.058	0.436	−0.536	−0.038	0.285
C (fingers)	0.197	12.1	0.096	0.069	−0.570	2.46	−20.1	−0.23	4.67

NOTE.—Cases A, B, and C represent the three possibilities found in numerical simulations, classified according to the criteria in eqs. (16) and (17).

In Figure 1 we plot the lines of critical stability given by equations (16) and (17) (*solid and dotted lines, respectively*) in the $\Delta\nabla T$-∇Y plane. The asterisks indicate the particular values of the gradients for each of the three cases considered, the parameters of which are summarized in Table 1. The shaded area covers the region in which all the roots of the cubic equation (13) are real. We denote by "neutron fingers" the region in which the condition in equation (16) is fulfilled, but not the condition in equation (17); by "convection" we denote those regions in which the conditions in both equations (16) and (17) are satisfied; we denote by "semiconvection" the case in which the condition in equation (17) is satisfied, but the condition in equation (16) is not.

By applying the Routh criterium (DiStefano et al. 1994), which states that the number of unstable modes of a cubic equation is given by the number of changes of sign in the sequence

$$\left\{1,\ a_2,\ \frac{a_2a_1 - a_0}{a_2},\ a_0\right\}, \tag{18}$$

we deduce that the number of unstable modes in the regions labeled by "convection" or "neutron finger" is always one. Thus, the root corresponding to this mode is real and positive. Notice that while in the convection case all roots are real, in the neutron-finger case, the two stable modes can be either real or complex conjugates. In the region labeled "semiconvection," we have two unstable modes, which may be either real or complex conjugates. "Semiconvection" can be, therefore, oscillatory (complex conjugate unstable modes) or nonoscillatory (two real unstable modes). We emphasize that the convention we use to divide the $\Delta\nabla T$-∇Y plane according to the instability criteria in equations (16) and (17) differs from that of Bruenn & Dineva (1996). According to their convention, the convectively unstable region is extended to contain that part of our neutron-finger and semiconvection regions in which all roots are real. In general, the classification in different types of instability is somehow arbitrary, because there is no clear qualitative distinction between neutron fingers and convection: in both cases, the unstable root is real. Our classification simply responds to the fact that in the limit of vanishing diffusivity, the criteria in equations (16) and (17) reduce to the classical Rayleigh-Taylor and Schwarzschild criteria, and it certainly is not the only valid choice. The important idea to bear in mind is that when all the kinetic coefficients are of similar magnitude, the distinction among the different types of instabilities is less evident, and only the concept of overall stability is meaningful.

3.2. *Magnetic PNSs*

In the general case, $\boldsymbol{B} \neq 0$, equation (18) can be rewritten as

$$\gamma^4 + q_3\gamma^3 + q_2\gamma^2 + q_1\gamma + q_0 = 0\ , \tag{19}$$

where

$$\begin{aligned} q_3 &= a_2 + \omega_m\ , \\ q_2 &= a_1 + \omega_m a_2 + \omega_{\rm A}^2\ , \\ q_1 &= a_0 + \omega_m a_1 + \omega_{\rm A}^2(\omega_T + \omega_Y)\ , \\ q_0 &= \omega_m a_0 + \omega_{\rm A}^2(\omega_T\omega_Y - \omega_{TY}\omega_{YT})\ . \end{aligned} \tag{20}$$

Equation (19) describes four essentially different modes that can generally exist in chemically inhomogeneous fluid in the presence of a magnetic field. The Routh criterium applied to a quartic equation states that the number of roots with a positive real part (unstable modes) is given by the number of changes of sign in the sequence

$$\left\{1,\ q_3,\ \frac{q_3q_2 - q_1}{q_3},\ q_1 - \frac{q_3^2q_0}{q_3q_2 - q_1},\ q_0\right\}. \tag{21}$$

Since q_3 is always positive, there is at least one stable mode. The criteria for hydromagnetic instability is equivalent to requiring that any one of the following inequalities be satisfied:

$$q_0 < 0\ , \tag{22}$$

$$q_3q_2 - q_1 < 0\ , \tag{23}$$

$$q_1 - \frac{q_3^2q_0}{(q_3q_2 - q_1)} < 0\ . \tag{24}$$

In general, the magnetic field has a stabilizing effect on all three conditions. Consequently, there is a critical value of $\boldsymbol{B}$ above which none of the instability conditions is fulfilled and all modes become stable.

To warm up, we begin analyzing the behavior of the roots with increasing magnetic field. In Figure 2 we draw a sketch, plotting the real part (γ) of the four modes as a function of $\omega_{\rm A}^2$. Modes with positive γ are unstable. In order to show more clearly the qualitative effect, we have assigned values

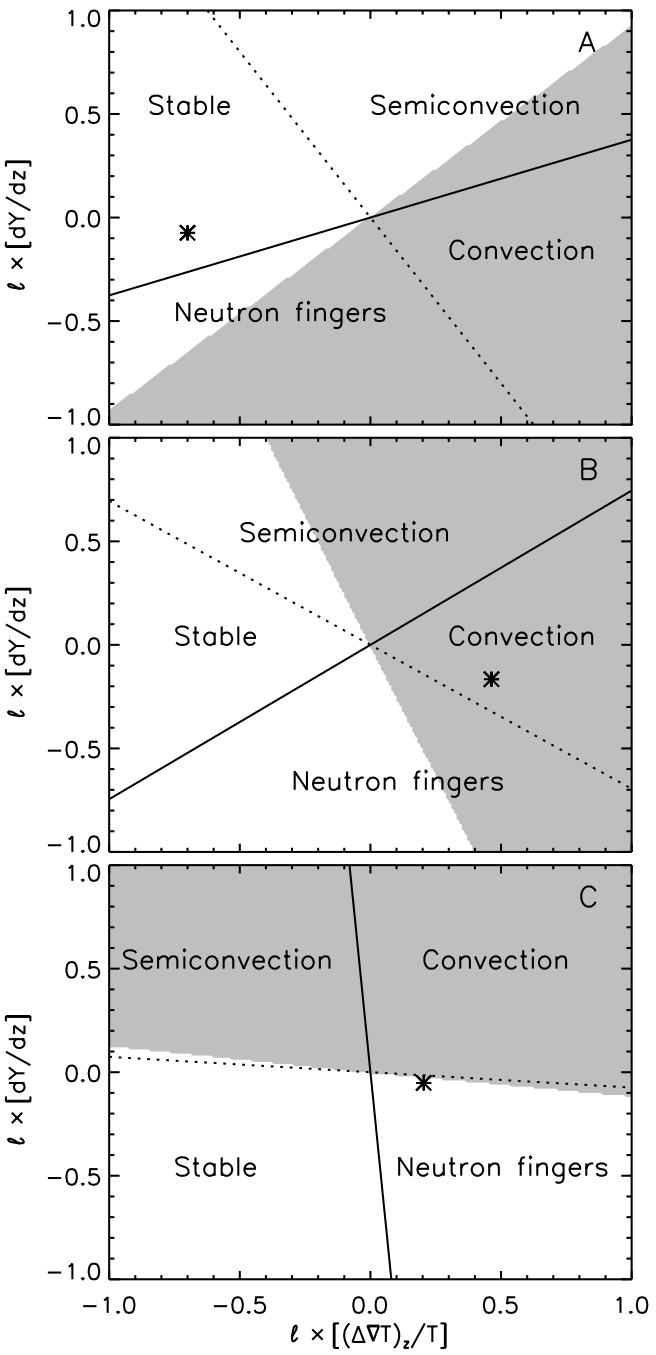

FIG. 1.—Stability plane for the three thermodynamic states detailed in Table 1. Four different regions in the plane are separated by the criteria in eqs. (16) and (17) (*solid and dotted lines, respectively*). The shaded area indicates the region in which the three roots of eq. (13) are real. The particular values of the gradients in each studied case (A, B, C) are indicated by asterisks. The scale factor *l* has been taken as the pressure height of each case.

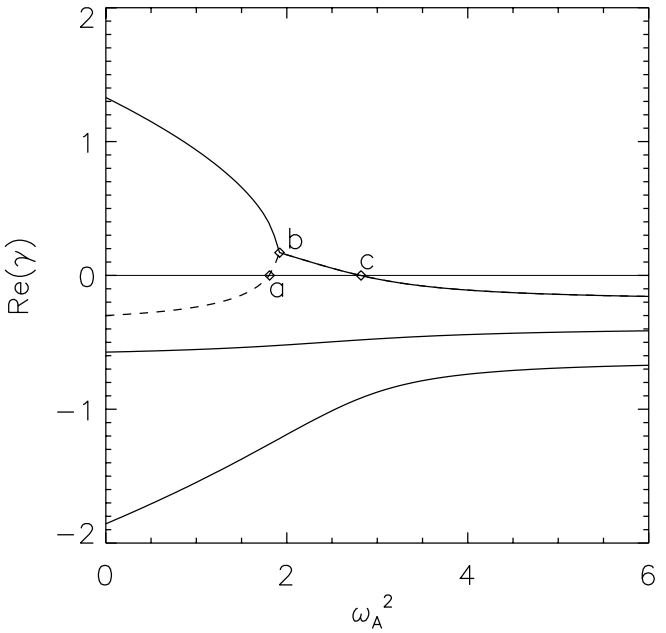

FIG. 2.—Sketch showing the behavior of the real part of the roots of eq. (19) as a function of the square of the Alfvén frequency, for fixed values of the dynamical and dissipative frequencies. The dashed line corresponds to the mode decoupled in the nonmagnetic case (referred to as "magnetic mode" in the text). Units are arbitrary and the points a, b, and c indicate changes of sign and character (real-complex) of the modes. See § 3.1 for further details.

to the dissipative frequencies that do not correspond to real values encountered in the early stages of a neutron star's life. The qualitative behavior using real coefficients is very similar, although the different scales would not allow one to capture the trends in a simple plot. In the limit of a vanishing magnetic field ($\omega_A \to 0$), there are three nonmagnetic modes (*solid lines*), discussed in the previous section, that remain essentially unaltered, and a stable magnetic mode with a value equal to $-\omega_m$ (*dashed line*). The situation shown in Figure 2 would correspond to the convection case (one unstable and two stable nonmagnetic modes when $\boldsymbol{B} = 0$). By switching on the magnetic field, the real part of the new magnetic mode (*dashed line*) increases and becomes positive at the point labeled a, which corresponds to the physical conditions such that $q_0 = 0$. At that point, the original unstable mode (*top solid line*) has been partially damped. Further increasing the magnetic field, the real parts of the originally unstable mode and the new unstable magnetic mode merge, to form a pair of complex conjugate modes (point b). Convection thus becomes oscillatory, due to the stabilizing action of the magnetic field. At a critical magnetic field, given by the condition in equation (24), the real part of the unstable modes vanishes (point c), and for a higher magnetic field, all modes are stable. The originally stable modes are not seriously affected.

The general trends discussed above (namely, damping of the unstable mode, a new magnetic mode becoming unstable, merging of modes and change to oscillatory convection, and final suppression of instabilities) are also found when realistic kinetic coefficients from numerical simulations are used. To quantify the characteristic values of the magnetic field causing the effects described above, we have taken the parameters corresponding to case B from Table 1. Those modes with a typical wavelength of the order of the pressure height (see below for further discussion), suffer the transitions a, b, and c in Figure 2 when $B = 2.5 \times 10^{11}$, 1.8×10^{16}, and 2.09×10^{16} G, respectively. Thus, a field larger than 2.09×10^{16} G entirely suppresses all types of instability in the considered region.

In order to understand the effect of the magnetic field on each instability condition, it is more convenient to rewrite equations (22)–(24) separating the terms containing the

Alfvén frequency and magnetic dissipation:

$$a_0 < -\frac{\omega_A^2}{\omega_m}(\omega_T\omega_Y - \omega_{TY}\omega_{YT}) , \quad (25)$$

$$a_2a_1 - a_0 < -\omega_m a_2(a_2 + \omega_m) - \omega_A^2(\omega_\nu + \omega_m) , \quad (26)$$

$$\left[a_0 + \omega_m a_1 + \omega_A^2(\omega_T + \omega_Y)\right] \times \left[a_2a_1 - a_0 + \omega_m a_2(a_2 + \omega_m) + \omega_A^2(\omega_\nu + \omega_m)\right] < (a_2 + \omega_m)^2\left[(\omega_m a_0 + \omega_A^2(\omega_T\omega_Y - \omega_{TY}\omega_{YT})\right] . \quad (27)$$

These inequalities can be further simplified if we take into account that the frequencies entering these conditions are of different orders of magnitude in PNSs. The dissipative frequencies ω_ν, ω_T, ω_Y, ω_{TY}, and ω_{YT} are approximately comparable to each other and range between 10–10^3 s^{-1}. The magnetic dissipative frequency ω_m is much smaller. The electrical resistivity of hot nuclear matter (R) is relatively low, $R \approx 6 \times 10^{-29} T_8^2$ s (Yakovlev & Shalybkov 1991); thus, the characteristic timescale of dissipation of the magnetic field is extremely long compared to other dissipative timescales. Taking into account that $\nu_m = c^2R/4\pi$, we can estimate $\omega_m \sim 10^{-11}$ s^{-1} for $k \sim \pi/l$. Therefore, we can neglect ω_m when it enters the conditions in equations (23) and (24) in a row with other dissipative frequencies. In addition, because of the small magnetic diffusivity, it also turns out that $\omega_m\omega_\nu \ll \omega_A^2$, and equation (22) can be written as

$$-\omega_g^2(\omega_Y - \alpha\omega_{YT}) - \omega_L^2\left(\omega_T - \frac{1}{\alpha}\omega_{TY}\right) + \frac{\omega_A^2}{\omega_m}(\omega_T\omega_Y - \omega_{TY}\omega_{YT}) < 0 . \quad (28)$$

All three conditions depend on the wavevector k. It is well known (Chandrasekhar 1961) that in the inviscid limit, the minimal values of gradients that can cause instability of a magnetized fluid correspond to $k \to \infty$. Taking account of viscosity increases the most unstable horizontal wavelength, and the critical gradients are reached for a large, although finite, value of k. In the case of low magnetic dissipation, k is much larger than π/d. Substituting $k \approx Q$ into equation (35), we have

$$\frac{dY}{dz}(\delta\kappa_T - \beta\kappa_Y) - \frac{\Delta\nabla T}{T}(\beta\lambda_Y - \delta\lambda_T) < -\frac{\pi B^2}{4g\rho d^2\nu_m}(\kappa_T\lambda_Y - \kappa_Y\lambda_T) . \quad (29)$$

Due to the particular physical conditions in PNSs ($\omega_m \ll 1$), even a relatively low magnetic field can make this condition not satisfied. We must point out, however, that this criterium is associated to the change of sign of the new magnetic mode (Fig. 2, *dashed line*), which is irrelevant, because the dominant unstable mode is always that associated with one of the other two conditions.

Let us turn back to the other two conditions, equations (26) and (27). The dissipative frequencies are usually small compared to the dynamical frequencies ω_g and ω_L for typical length scales in a PNS. For example, the contribution of terms proportional to the cube of dissipative frequencies in equations (26) and (27) does not exceed 10%. Therefore, we can neglect the terms containing only dissipative frequencies compared to those containing the dynamical ones (including the Alfvén frequency). This latter approximation is justified if the magnetic field is large enough for ω_A to be larger than any dissipative frequency, $\omega_A > \omega_{diss} = \max(\omega_\nu, \omega_T, \omega_Y, \omega_{TY}, \omega_{YT})$. Since $\omega_{diss} \sim 0.1$–1 s^{-1}, the condition $\omega_A > \omega_{diss}$ is fulfilled if the magnetic field exceeds some characteristic value that is of the order of 10^{12}–10^{13} G. For $B < 10^{13}$ G, the influence of the magnetic field is insignificant, and the conditions in equations (26) and (27) are exactly equivalent to the conditions in equations (16) and (17). For $B > 10^{13}$ G, the instability conditions can be simplified as

$$-\omega_g^2(\omega_Y - \alpha\omega_{YT}) - \omega_L^2\left(\omega_T - \frac{\omega_{TY}}{\alpha}\right) + \omega_A^2(\omega_T + \omega_Y) < 0 , \quad (30)$$

$$-\omega_g^2(\omega_T + \omega_\nu + \alpha\omega_{YT}) - \omega_L^2\left(\omega_Y + \omega_\nu + \frac{\omega_{TY}}{\alpha}\right) + \omega_\nu\omega_A^2 < 0 . \quad (31)$$

As for equation (28), the minimal values of the gradients that cause the instability correspond to $k \approx Q$ (short wavelengths). Substituting $k = Q$ into equations (30) and (31), we have

$$\frac{dY}{dz}(\delta\kappa_T - \beta\kappa_Y) - \frac{\Delta\nabla T}{T}(\beta\lambda_Y - \delta\lambda_T) < -\frac{\pi B^2}{4g\rho d^2}(\kappa_T + \lambda_Y) , \quad (32)$$

$$\frac{dY}{dz}[\delta(\nu + \lambda_Y) + \beta\kappa_Y] - \frac{\Delta\nabla T}{T}[\beta(\nu + \kappa_T) + \delta\lambda_T] < -\frac{\pi\nu B^2}{4g\rho d^2} . \quad (33)$$

Note that these criteria are analogous to the instability criteria for nonmagnetic PNSs in equations (16) and (17), but replacing

$$\nu(\kappa_T\lambda_Y - \kappa_Y\lambda_T) \to \frac{d^2B^2}{27\pi^3\rho}(\kappa_T + \lambda_Y) , \quad (34)$$

$$(\kappa_T + \lambda_Y)[(\nu + \kappa_T)(\nu + \lambda_Y) - \lambda_T\kappa_Y] \to \frac{d^2B^2}{27\pi^3\rho}\nu , \quad (35)$$

and the magnetic field plays the role of an efficient dissipative process. In magnetic PNSs, the dissipative effect caused by the Lorentz force is much greater than neutrino transport or neutrino viscosity effects.

In Figure 3 we show the unstable zones at each time of the evolution of a young PNS from one of the numerical simulations in Pons et al. (1999). Top and bottom panels correspond to the criteria in equations (32) and (33), respectively. The criterion in equation (33) depends on the neutrino viscosity, for which available estimates are sometimes contradictory (van den Horn & van Weert 1981; Goodwin & Pethick 1982; Thompson & Duncan 1993). In our simulations we used the value $\nu = \eta^2\kappa_T$ (van den Horn & van Weert 1981). The contours indicate the convectively unstable region for the following values of a passive magnetic field: 10^{14} (*solid line*), 5×10^{15} (*dotted line*), 10^{16} (*dashed line*), 3×10^{16} (*dash-dotted line*), and 5×10^{16} G (*dash–triple-dotted line*). It turns out that with this viscosity, the critical magnetic fields for the criteria in equations (32) and (33) are of the same order of magnitude. The magnetic cor-

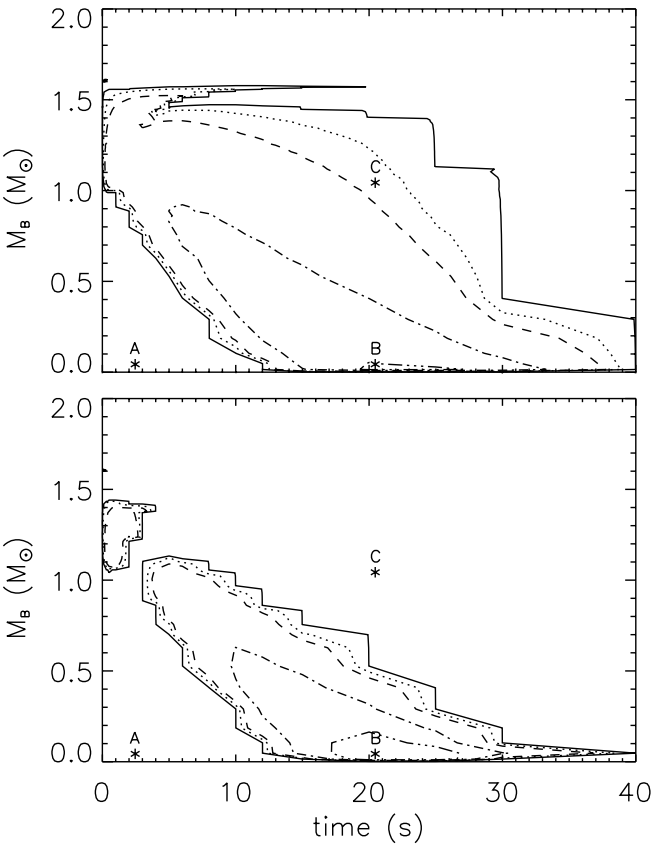

FIG. 3.—Contour plots showing the variation of the different convectively unstable zones, assuming different strengths of the magnetic field. The contour lines correspond to the following values of the magnetic field: 10^{14} (*solid line*), 5×10^{15} (*dotted line*), 10^{16} (*dashed line*), 3×10^{16} (*dash-dotted line*), and 5×10^{16} G (*dash–triple-dotted line*). The top panel refers to the unstable region according to criteria in eq. (32) and the bottom panel refers to eq. (33). The *x*-axis indicates the evolution time and the *y*-axis the enclosed baryonic mass of the layer. The innermost part of the star remains unstable at intermediate times, even when magnetic fields as large as 10^{16} G are present. The asterisks correspond to the cases A, B, and C described in the text. This PNS model was taken from numerical simulations performed in Pons et al. (1999).

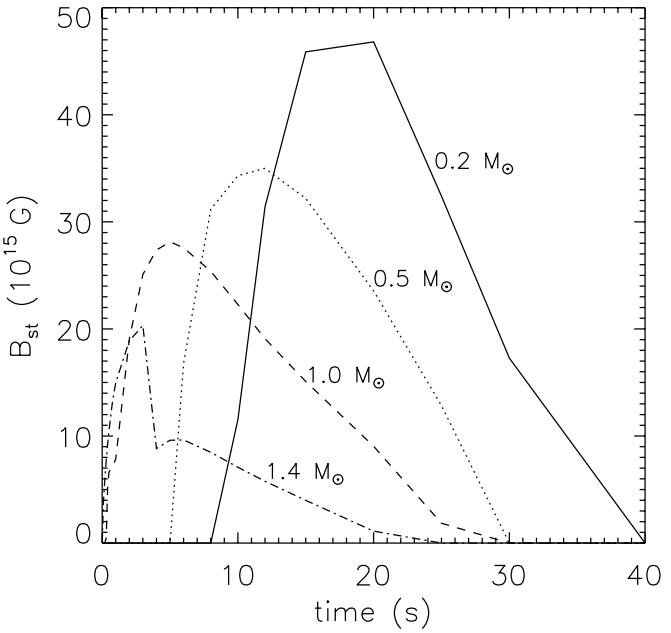

FIG. 4.—Critical magnetic field strength that completely stabilizes the fluid as a function of the evolution time. The four lines stand for four different layers, with enclosed baryonic masses of 0.2 (*solid line*), 0.5 (*dotted line*), 1.0 (*dashed line*), and 1.4 (*dash-dotted line*) $M_\odot$, respectively. The PNS model is the same as in Fig. 3. In general, the deeper the layer is, the larger the magnetic field required for unconditional stabilization.

rection for equation (33) is somewhat more restrictive, and generally, its associated instability is suppressed with weaker magnetic fields. The difference is caused mainly by the different combinations of kinetic coefficients that appear in the equations. Both criteria require a rather strong magnetic field, $B \sim (1\text{–}5) \times 10^{16}$ G, in order to stabilize the fluid completely, although the region in which the condition in equation (33) is fulfilled is typically smaller than that given by the condition in equation (32). Note that moderate magnetic fields of the order of $\leq 10^{14}$ G leave the unstable regions essentially unchanged, and the effects are visible only for $B \geq 10^{15}$ G.

In Figure 4 we plot the critical magnetic field ($B_{\rm st}$) that completely stabilizes a certain layer of the PNS (corresponding to enclosed baryonic masses of 0.2, 0.5, 1.0, and 1.4 $M_\odot$) as a function of time. Layers with $M_B < 1\ M_\odot$ are stable at the beginning of the evolution. Later on, when the corresponding layer becomes unstable, $B_{\rm st}$ grows rapidly, reaching some maximum value, and then decreases monotonically as the temperature and lepton gradients are smeared out via neutrino diffusion. The maximum value of $B_{\rm st}$ at different points varies in a very narrow range $(2\text{–}5) \times 10^{16}$ G, but this maximum is reached at different instants in time. Note that $B_{\rm st}$ provides stabilization in the largest unstable length scale. Stabilization at smaller scales is accomplished with weaker magnetic fields. The instability seems to be especially persistent in the central region with $M_B < 0.5\ M_\odot$, in which convective motions might last for a long time (Keil et al. 1996) and $B_{\rm st} \sim 5 \times 10^{16}$ G.

4. DISCUSSION

In this paper we have considered the effect of the magnetic field (consistently coupled to other dissipative processes, such as neutrino transport and neutrino viscosity) on the convective instability of PNSs. Our results show that transport phenomena play an important role in determining the size of the region of the star that is subject to instability. The particular values of the transport and kinetic coefficients also determine the kinds of instabilities that can be present in an unstable region (convection, neutron fingers, semiconvection).

For low magnetic fields ($B < 10^{13}$ G), the region where instabilities are present remains unaffected when compared to the nonmagnetic case. That region covers an important part of the PNS and lasts for almost the whole Kelvin-Helmholtz phase of the PNS evolution. Consequently, because of the existence of such an extended region subject to instabilities, convective motions are likely to appear and turbulent dynamo action can significantly increase the local magnetic field strength.

Once the magnetic field has a significant strength (10^{13} G $< B < 10^{15}$ G), its effect is twofold. First, it is responsible for the appearance of a new mode, which can generally be unstable, although in this case, its growth time is always longer than that of the other unstable modes. Sec-

ond, the magnetic field acts as a stabilizing agent for all types of instability studied in the nonmagnetic case, progressively reducing the size of the convective regions. Our calculations show, however, that only a relatively strong magnetic field can significantly influence the stability properties of PNSs, particularly in the central region with $M_B < 0.5\ M_\odot$. For instance, if the dynamo action is sufficiently efficient, the duration of the convective epoch can be noticeably shorter as the magnetic field increases up to $\geq 10^{16}$ G. We find that the critical magnetic field that suppresses all sorts of instability happens to be in a narrow range, at about 5×10^{16} G. This can be considered as an upper limit to the poloidal magnetic field generated by a convective dynamo.

In our simplified approach, we have considered the case of a vertical magnetic field. It is known (Chandrasekhar 1961) that this magnetic configuration requires the maximal field strength for stabilization. In real conditions, the field geometry may be more complex, with a substantial component perpendicular to the temperature and composition gradients. In PNSs, this field component can correspond, for example, to a toroidal magnetic field. For this geometry, the stabilizing magnetic field is typically several times lower. Therefore, stabilization against hydromagnetic instabilities can really take place at a slightly weaker magnetic field than that obtained in our calculations. In the presence of differential rotation (a very likely situation after the core collapse), the main contribution to the total field strength would be given by the toroidal magnetic field (B_t), and the poloidal component (B_p) would be less important. In a quasi-stationary regime, the rate of stretching of the toroidal field lines from the poloidal configuration by differential rotation is compensated by turbulent dissipation (Parker 1979). By equating both rates, one can write the following equation,

$$\frac{B_p}{\tau} \sim \frac{v_T l_T}{3} \nabla^2 B_t \ , \tag{36}$$

where τ is the characteristic stretching time, v_T the turbulent velocity, and l_T the turbulent length scale. Since the stretching is due to differential rotation, τ might be estimated as $\tau = |\Delta\Omega|^{-1}$, $\Delta\Omega$ being the difference between the maximum and minimum angular velocity. An estimation of $\nabla^2 B_t$ is $\sim B_t/R^2$, R being the typical radius of the star. Using the values $R \sim 20$ km, $v_T \sim 10^8$ cm s^{-1}, and $l_T \sim 10^5$ cm, we obtain

$$\frac{B_t}{B_p} \sim \frac{\Delta\Omega}{1\ \mathrm{s}^{-1}} \ . \tag{37}$$

Assuming that neutron stars are born with large angular velocities (say $\Omega = 10^3$ s^{-1}) and that $\Delta\Omega/\Omega$ is comparable to that of the Sun (0.1–0.3), we can estimate the toroidal field to be $\approx$100–300 times stronger than the poloidal component. Since the total magnitude of the magnetic field generated by dynamo action should not exceed, in any case, 10^{16} G, we have to conclude that the poloidal component that may represent the observed pulsar field must be in the range 3×10^{13}–10^{14} G. This estimate is in agreement with the observed fields of young pulsars in supernova remnants. The toroidal field could be, however, much stronger, which might lead to important consequences for the structure of neutron stars (Bocquet et al. 1995; Cardall, Prakash, & Lattimer 2001).

This work was supported by the Spanish Ministerio de Ciencia y Tecnología (grant AYA 2001-3490- C02-02), the EU Program "Improving the Human Research Potential and Socio-Economic Knowledge Base" (Research Training Network contract HPRN-CT-2000-00137), the Russian Foundation of Basic Research, and Deutsche Forschungsgemeinschaft (grant 00-02-04011). V. U. also thanks the Ministerio de Educacion, Cultura, y Deporte of Spain for financial support under the grant SAB 1999-0222. J. P. is supported by the Marie Curie fellowship HPMF-CT-2001-01217. The authors acknowledge an anonymous referee for useful suggestions.

REFERENCES

Aleksandrov, A. D., Kolmogorov, A. N., & Laurentiev, M. A. 1985, Mathematics: Its Content, Methods, and Meaning (Cambridge: MIT Press)
Ardelyan, N., Bisnovatyi-Kogan, G., & Popov, Y. 1980, Soviet Astron., 23, 705
Bocquet, M., Bonazzola, S., Gourgoulhon, E., & Novak, J. 1995, A&A, 301, 757
Bruenn, S., & Dineva, T. 1996, ApJ, 458, L71
Bruenn, S., & Mezzacappa, A. 1994, ApJ, 433, L45
———. 1995, Phys. Rep., 256, 69
Burrows, A., & Fryxell, B. 1993, ApJ, 418, L33
Burrows, A., & Lattimer, J. M. 1986, ApJ, 307, 178
Burrows, A., Young, T., Pinto, P., Eastman, R., & Thompson T. A. 2000, ApJ, 539, 865
Cardall, C. Y., Prakash, M., & Lattimer, J. M. 2001, ApJ, 554, 322
Chandrasekhar, S. 1961, Hydrodynamic and Hydromagnetic Stability (Oxford: Clarendon)
DiStefano, J. J., III, Stubberud, A. R., & Williams, I. J. 1994, Schaum's Outline of Theory and Problems of Feedback and Control Systems (New York: McGraw-Hill)
Epstein, R. 1979, MNRAS, 188, 305
Ginzburg, V. 1964, Dokl. Akad. Nauk SSSR, 156, 43
Ginzburg, V., & Ozernoy, L. 1964, Soviet Phys.–ZhETF, 47, 1030
Goodwin, B. T., & Pethick, C. J. 1982, ApJ, 253, 816
Janka, H.-Th. 2000, Nucl. Phys. A, 663, 119
Janka, H.-Th., & Müller, E. 1996, A&A, 306, 167
Keil, W., & Janka, H.-T. 1995, A&A, 296, 145
Keil, W., Janka, H.-Th., & Müller, E. 1996, ApJ, 473, L111
Landau, L. D., & Lifshitz, E. M. 1987, Fluid Mechanics (New York: Pergamon)
Liebendorfer, M., et al. 2001, Phys. Rev. D, 63, 103004
Miralles, J. A., Pons, J. A., & Urpin, V. 2000, ApJ, 543, 1001 (MPU00)
Parker, E. N. 1979, Cosmical Magnetic Fields: Their Origin and Their Activity (Oxford: Oxford Univ. Press)
Pons, J. A., Miralles, J. A., Prakash, M., & Lattimer, J. M. 2001a, ApJ, 553, 382
Pons, J. A., Reddy, S., Prakash, M., Lattimer, J. M., & Miralles, J. A. 1999, ApJ, 513, 780
Pons, J. A., Steiner, A. W., Prakash, M., & Lattimer, J. M. 2001b, Phys. Rev. Lett., 86, 5223
Rampp, M., & Janka, H.-Th. 2000, ApJ, 539, L33
Shapiro, S., & Teukolsky, S. 1983, Black Holes, White Dwarfs, and Neutron Stars (New York: Wiley)
Thompson, C., & Duncan, R. 1993, ApJ, 408, 194
Thompson, C., & Murray, N. 2001, ApJ, 560, 339
van den Horn, L. J., & van Weert, Ch. G. 1981, ApJ, 251, L97
Woltjer, L. 1964, ApJ, 140, 1309
Yakovlev, D., & Shalybkov, D. 1991, Ap&SS, 176, 2
Zeldovich, Ya., & Novikov, I. 1971, Stars and Relativity (Chicago: Univ. Chicago Press)